

Subspace Identification Methods and Multivariable Control for a Doubly-fed Induction Generator

Danna L. Albarracín Ávila
 Electrical Engineering
 Universidad Tecnológica de Pereira
 Pereira, Colombia
 Email: dlabarracin@utp.edu.co

Eduardo Giraldo
 Department of Electrical Engineering
 Universidad Tecnológica de Pereira
 Pereira, Colombia
 Email: egiraldos@utp.edu.co

Abstract—Doubly-Fed Induction Generators (DFIG) are being widely used on Wind Turbine Generator System (WTGS), although synchronous generators are being extensively utilized too. Thus, there are different types of identification techniques to obtain an estimated model of system. Orthogonal Decomposition (ORT) and Multivariable Output Error State Space (MOESP) algorithms are two well-known subspace identification techniques, discussed in this paper. These identification techniques are often implemented for multivariable systems. Subspace identification algorithms are attractive since the state space form is highly suitable to estimate, predict, filters, as well as for control design. The Doubly-Fed Induction Generator is widely used in the variable-speed constant-frequency Wind Power Generation System, using the vector control scheme which provides good performance in maximum wind energy capturing. In the traditional vector control scheme, the reduced doubly-fed induction generator model, which neglects the stator flux transients, is employed to simplify the rotor current inner-loop controller using the standard Proportional-Integral (PI) regulation. The approach proposed in this paper must be approached in order to obtain an approximate model influenced by the behaviour of the system with certain functional characteristics and environmental changes.

Keywords-subspace identification; parameters estimated; wind turbine; multivariable system; integral controller.

I. INTRODUCTION

Subspace identification methods have proven to be such a valuable tool in identification area since past few years. This interest is due to the ability of the subspace approach in providing accurate state-space models for multivariable linear systems directly from input-output data [1][2]. In the identification procedure, the main step is to compute the Singular Value Decomposition (SVD) of a block Hankel matrix H [3] constructed with input-output data. The computation of SVD can be done offline or online. The offline can be easily converted to an adaptive online version for a slow time Vaihingen system, such as process control system [3]-[4].

In control systems design with advanced model-based control methods, lots of time and cost are required for system identification to construct accurate models like a variable-speed induction machine. To save the cost for modeling of dynamical systems, it is important to choose proper test signals so that the leading dynamics are

stimulated efficiently [5]. A doubly-fed induction generator is a variable-speed induction machine widely utilized in the modern wind power industry. The reasons for using variable speed wind turbines are fourfold: 1) a higher energy yield, 2) a reduction of mechanical loads and a simpler pitch control, 3) an extensive controllability of both active and reactive powers, and 4) less fluctuation in output power [5][6].

There are several vector control strategies for a wind turbine driven DFIG's; one common method is to control the rotor current with Stator Flux Orientation (SFO) [7]. In all the existing control schemes, the reduced DFIG model, which neglects the transient terms in the stator flux and most of them use the traditional PI regulator in their rotor current controllers [8].

In this paper, two subspace approaches are observed in order to perform open-loop system identification. These two approaches are the Orthogonal Decomposition (ORT) method and Multivariable Output Error State Space (MOESP) method. The objective of this paper is to analyse the performance of the models in identifying the state space model of a doubly-fed induction generator (DFIG) and the performance of the Integral multivariable controller applied to the estimated system, as shown in Section 3 and Section 4, respectively.

II. MODELING OF DFIG

A. General Descriptions

Figure 1 illustrates the DFIG wind power generation system consisting of a wound rotor induction generator and a back-to-back converter between the rotor slip rings and the grid.

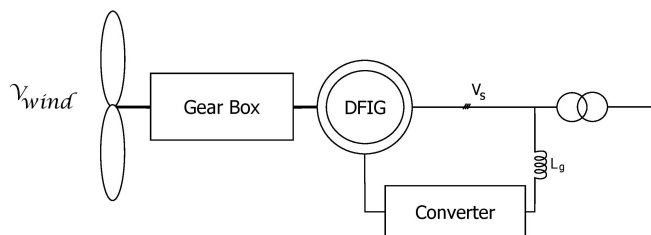


Figure 1. Variable-speed wind turbine system using DFIG.

B. Mathematical Model of DFIG

Figure 2 shows the equivalent circuit of a DFIG in the reference frame rotating at the synchronous angular speed ω_1 [7].

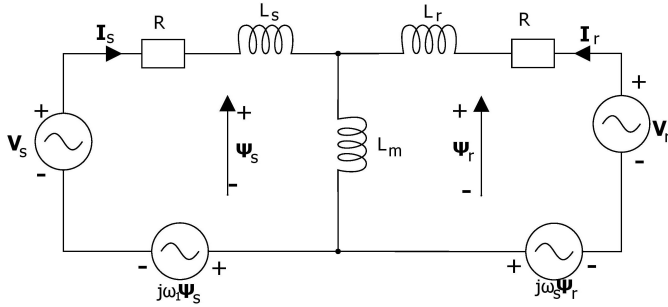


Figure 2. T-equivalent circuit of DFIG in reference frame rotating at ω_1 .

According to Figure 2, the stator and rotor space-vector fluxes Ψ_s and Ψ_r are given respectively by

$$\begin{cases} \Psi_s = L_s \mathbf{I}_s + L_m \mathbf{I}_r \\ \Psi_r = L_m \mathbf{I}_s + L_r \mathbf{I}_r \end{cases} \quad (1)$$

where $L_{\sigma s}$, $L_{\sigma r}$ and L_m are the stator and rotor leakage and mutual inductances, and $L_s = L_{\sigma s} + L_m$ and $L_r = L_{\sigma r} + L_m$ the self inductances of the stator and rotor windings, respectively.

The stator and rotor space-vector voltages \mathbf{V}_s and \mathbf{V}_r in the same reference frame can be expressed as

$$\begin{cases} \mathbf{V}_s = R_s \mathbf{I}_s + \frac{d\Psi_s}{dt} + j\omega_1 \Psi_s \\ \mathbf{V}_r = R_r \mathbf{I}_r + \frac{d\Psi_r}{dt} + j(\omega_1 - \omega_r) \Psi_r \end{cases} \quad (2)$$

where \mathbf{I}_s and \mathbf{I}_r are the stator and rotor current vectors, \mathbf{R}_s and \mathbf{R}_r the stator and rotor resistances, ω_r is the rotor angular speed, and $\omega_s = \omega_1 - \omega_r$ the slip angular speed.

The model of DFIG uses the SVO scheme described in [7], in which we can rewrite the rotor voltage equation in the synchronous $d-q$ reference frame as

$$\begin{cases} \mathbf{V}_{rd} = V'_{rd} + \frac{L_m}{L_s} \left(\mathbf{V}_s - \frac{R_s}{L_s} \Psi_{sd} + \omega_r \Psi_{sq} \right) \\ \mathbf{V}_{rq} = V'_{rq} - \frac{L_m}{L_s} \left(\frac{R_s}{L_s} \Psi_{sq} + \omega_r \Psi_{sd} \right) \end{cases} \quad (3)$$

where

$$\begin{cases} \mathbf{V}'_{rd} = R'_r \mathbf{I}_{rd} + \sigma L_r \frac{d\mathbf{I}_{rd}}{dt} - \omega_s \sigma L_r \mathbf{I}_{rq} \\ \mathbf{V}'_{rq} = R'_r \mathbf{I}_{rq} + \sigma L_r \frac{d\mathbf{I}_{rq}}{dt} + \omega_s \sigma L_r \mathbf{I}_{rd} \end{cases} \quad (4)$$

The system in state space representation is presented as

follows:

$$\begin{aligned} \frac{d\mathbf{I}_{rd}}{dt} &= \frac{1}{\sigma L_r} \left(V'_{rd} - R'_r \mathbf{I}_{rd} + \omega_s \sigma L_r \mathbf{I}_{rq} \right) \\ \frac{d\mathbf{I}_{rq}}{dt} &= \frac{1}{\sigma L_r} \left(V'_{rq} - R'_r \mathbf{I}_{rq} - \omega_s \sigma L_r \mathbf{I}_{rd} \right) \end{aligned} \quad (5)$$

$$\mathbf{y} = \begin{bmatrix} 1 & 0 \\ 0 & 1 \end{bmatrix} \begin{bmatrix} \mathbf{I}_{rd} \\ \mathbf{I}_{rq} \end{bmatrix}$$

III. SUBSPACE IDENTIFICATION METHOD

The model presented in Section 2 is nonlinear. The linear model of the DFIG can be obtained by applying an subspace approach as the ORT (Orthogonal Decomposition) or MOESP (Multivariable Output Error State Space) methods to the system around an operating point [3], as follows:

$$\begin{aligned} \mathbf{x}[k+1] &= \mathbf{A}\mathbf{x}[k] + \mathbf{B}\mathbf{u}[k] \\ \mathbf{y}[k] &= \mathbf{C}\mathbf{x}[k] + \mathbf{D}\mathbf{u}[k] \end{aligned} \quad (6)$$

being $\mathbf{x} \in \mathbb{R}^{n \times 1}$, where $n = 6$ is the number of state variables, $\mathbf{A} \in \mathbb{R}^{n \times n}$, $\mathbf{B} \in \mathbb{R}^{n \times p}$, where $p = 2$ is the number of inputs, $\mathbf{u} \in \mathbb{R}^{p \times 1}$, and $\mathbf{C} \in \mathbb{R}^{m \times n}$, where $m = 2$ is the number of outputs.

Suppose that the input-output data $\{u(t), y(t), t = 0, 1, \dots, N + 2k - 2\}$ are given with N sufficiently large and $k > n$. Based on the input-output data [1], we define as usual block Hankel matrices of past input is defined as

$$U_p = \begin{bmatrix} u(0) & u(1) & \cdots & u(N-1) \\ u(1) & u(2) & \cdots & u(N) \\ \vdots & \vdots & \ddots & \vdots \\ u(k-1) & u(k) & \cdots & u(N+k-2) \end{bmatrix} \quad (7)$$

and future input as

$$U_f = \begin{bmatrix} u(k) & u(k+1) & \cdots & u(k+N-1) \\ u(k+1) & u(k+2) & \cdots & u(k+N) \\ \vdots & \vdots & \ddots & \vdots \\ u(2k-1) & u(2k) & \cdots & u(N+2k-2) \end{bmatrix} \quad (8)$$

where $U_p, U_f \in \mathbb{R}^{km \times N}$. Similarly, we define past and future output $Y_p, Y_f \in \mathbb{R}^{kp \times N}$ respectively. In [9], the constructed input and output are given as

$$U = \begin{bmatrix} U_p \\ U_f \end{bmatrix}, Y = \begin{bmatrix} Y_p \\ Y_f \end{bmatrix} \quad (9)$$

The extended observability matrix of order i is defined as

$$\Gamma_i = [C^T \quad (CA)^T \quad \cdots \quad (CA^{i-1})^T]^T \quad (10)$$

and the block lower triangular Toeplitz matrix as

$$H_i = \begin{bmatrix} D & 0 & \cdots & 0 \\ CB & D & \cdots & 0 \\ \vdots & \vdots & \ddots & \vdots \\ CA^{i-2}B & CA^{i-3}B & \cdots & D \end{bmatrix} \quad (11)$$

we consider a related LQ decomposition

$$\begin{bmatrix} U_f \\ U_p \\ Y_p \\ Y_f \end{bmatrix} = \begin{bmatrix} L_{11} & 0 & 0 & 0 \\ L_{21} & L_{22} & 0 & 0 \\ L_{31} & L_{32} & L_{33} & 0 \\ L_{41} & L_{42} & L_{43} & L_{44} \end{bmatrix} \begin{bmatrix} Q_1^T \\ Q_2^T \\ Q_3^T \\ Q_4^T \end{bmatrix} \quad (12)$$

Step 1: Construct data matrices of U_p, U_f, Y_p and Y_f

Step 2: Perform LQ factorization by (12)

Step 3: Perform SVD to the working matrix

ORT: $G = [L_{42}]$

MOESP: $G = [L_{42}L_{43}]$

where

$$G = \begin{bmatrix} \hat{U} & \bar{U} \end{bmatrix} \begin{bmatrix} \hat{S} & 0 \\ 0 & \bar{S} \end{bmatrix} \begin{bmatrix} \hat{V} \\ \bar{V} \end{bmatrix} \simeq \hat{U} \hat{S} \hat{V}^T$$

Step 4: Compute the estimates of A and C by (10)

$$\Gamma_i = \hat{U} \hat{S}^{1/2}$$

Step 5: Compute the estimates of B and D by (11)

$$\bar{U}^T L_{41} L_{11}^{-1} = \bar{U}^T H_i$$

IV. MULTIVARIABLE CONTROL

A. Integral multivariable controller

In Figure 3, the controller structure is defined by considering accumulated for the error in the signal control [10] is shown.

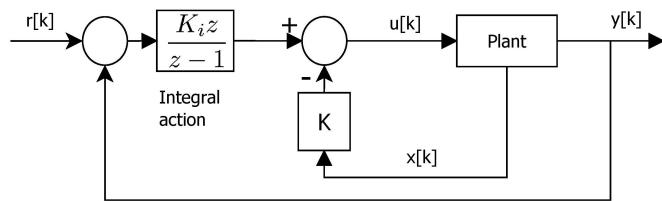


Figure 3. Block diagram of the integral action controller.

In [11], the error in the signal control is defined as follows

$$\mathbf{u}[k] = -\mathbf{K}\mathbf{x}[k] + \mathbf{K}_i\mathbf{v}[k] \quad (13)$$

with

$$\mathbf{v}[k+1] = \mathbf{v}[k] + \mathbf{e}[k] \quad (14)$$

where the error $\mathbf{e}[k]$ is defined as follows

$$\mathbf{e}[k] = \mathbf{r}[k] - \mathbf{y}[k] \quad (15)$$

and $\mathbf{v}[0] = 0$. Therefore, an extended system can be defined as follows

$$\begin{bmatrix} \mathbf{x}[k+1] \\ \mathbf{v}[k+1] \end{bmatrix} = \begin{bmatrix} \mathbf{A} & \mathbf{0} \\ -\mathbf{C} & \mathbf{I} \end{bmatrix} \begin{bmatrix} \mathbf{x}[k] \\ \mathbf{v}[k] \end{bmatrix} + \begin{bmatrix} \mathbf{B} \\ -\mathbf{D} \end{bmatrix} \mathbf{u}[k] + \begin{bmatrix} \mathbf{0} \\ -\mathbf{I} \end{bmatrix} \mathbf{r}[k] \quad (16)$$

$$\mathbf{y}[k] = \begin{bmatrix} \mathbf{C} & \mathbf{0} \end{bmatrix} \begin{bmatrix} \mathbf{x}[k] \\ \mathbf{v}[k] \end{bmatrix} \quad (17)$$

where the control signal is computed as follows

$$\mathbf{u}[k] = - \begin{bmatrix} \mathbf{K} & -\mathbf{K}_i \end{bmatrix} \begin{bmatrix} \mathbf{x}[k] \\ \mathbf{v}[k] \end{bmatrix} \quad (18)$$

V. RESULTS

The parameters of the doubly-fed induction generator used in the simulations are $R_s = 0.01(p.u.)$, $R_r = 0.009(p.u.)$, $L_{\sigma r} = 0.18(p.u.)$, $L_{\sigma s} = 0.07(p.u.)$, $L_m = 3.015(p.u.)$ and $\omega_s = 1.2(p.u.)$.

The wind energy conversion system is identified from behavior shown in Figure 4 and Figure 5. The estimated model by the ORT and MOESP method are shown in (19) and (20), respectively.

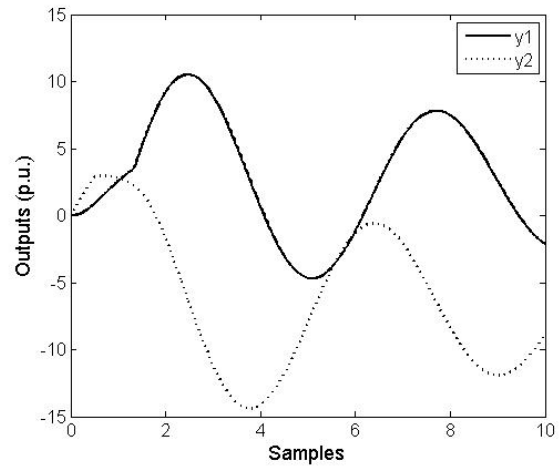


Figure 4. Output behavior.

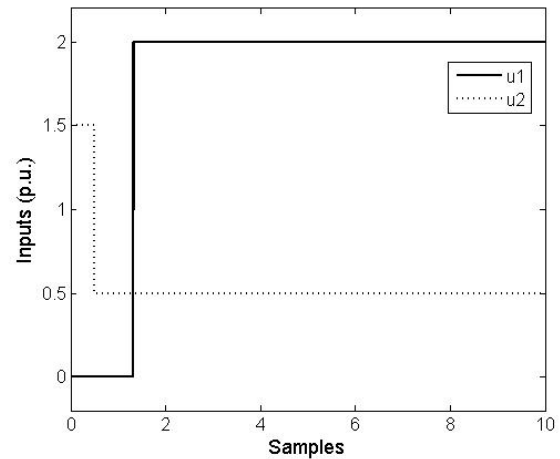


Figure 5. Input behavior.

$$\begin{aligned}
 \mathbf{A} &= \begin{bmatrix} 0.9992 & 0.0021 \\ -0.0684 & 0.9992 \end{bmatrix} & \mathbf{B} &= \begin{bmatrix} -0.0179 & 0.0007 \\ -0.0026 & -0.1041 \end{bmatrix} \\
 \mathbf{C} &= \begin{bmatrix} -2.3294 & -0.0199 \\ 0.1133 & -0.4085 \end{bmatrix} & \mathbf{D} &= \begin{bmatrix} 0.0594 & -0.0790 \\ 0.0054 & 0.0165 \end{bmatrix}
 \end{aligned} \tag{19}$$

$$\begin{aligned}
 \mathbf{A} &= \begin{bmatrix} 0.9992 & 0.0112 \\ -0.0129 & 0.9992 \end{bmatrix} & \mathbf{B} &= \begin{bmatrix} -0.0566 & 0.0620 \\ -0.1034 & -0.0494 \end{bmatrix} \\
 \mathbf{C} &= \begin{bmatrix} -0.2080 & -0.2871 \\ 0.3077 & -0.1940 \end{bmatrix} & \mathbf{D} &= \begin{bmatrix} 0.0467 & -0.2088 \\ 0.0014 & -0.0063 \end{bmatrix}
 \end{aligned} \tag{20}$$

The graph of superimpose between simulated true system data and simulated outputs obtained from ORT and MOESP models are shown in Figure 6 and Figure 7. The input data system is shown in Figure 8. In Figure 6 and Figure 7, the

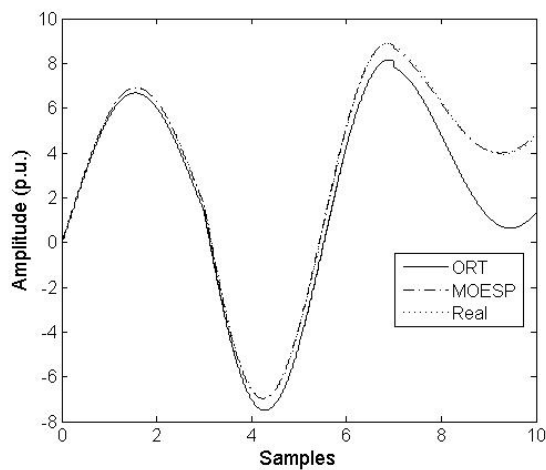


Figure 6. Superimpose between simulated true data system of output 1 and simulated output 1 obtained from estimated system matrices of ORT and MOESP methods.

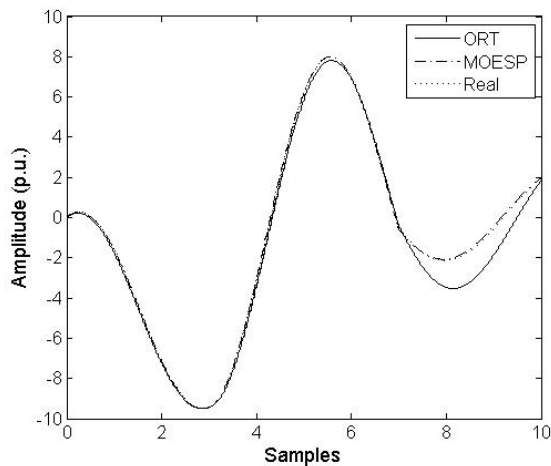


Figure 7. Superimpose between simulated true data system of output 2 and simulated output 2 obtained from estimated system matrices of ORT and MOESP methods.

MOESP method gives the best performance overall in open loop compared to the ORT model over the real response of system.

In Figure 9, Figure 10 and Figure 11, the outputs tracking performance and the control inputs are shown using the ORT model.

In Figure 12, Figure 13 and Figure 14, the outputs tracking performance and the control inputs are shown using the MOESP model.

As shown in Figure 14, the results for the control inputs by using the ORT method is better than the obtained results shown in Figure 11, the MOESP method, in terms of control signal amplitude.

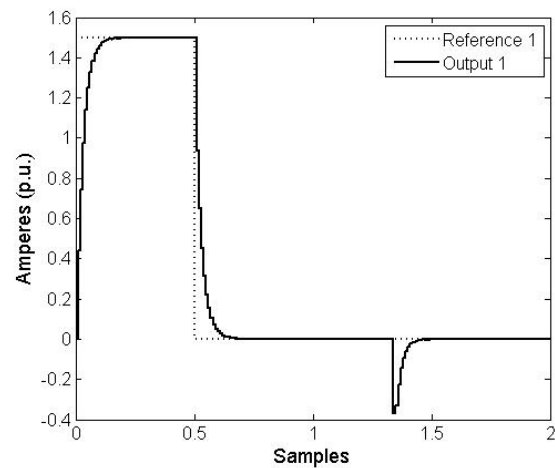


Figure 9. Output 1 tracking performance of ORT model by using integral multivariable controller.

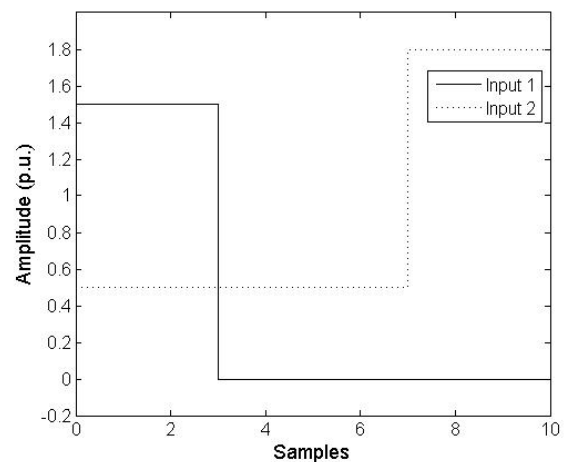


Figure 8. Input data of true system and estimated system matrices of ORT and MOESP methods.

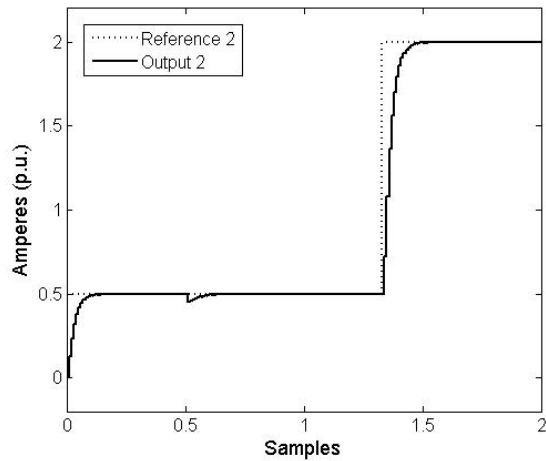


Figure 10. Output 2 tracking performance of ORT model by using integral multivariable controller.

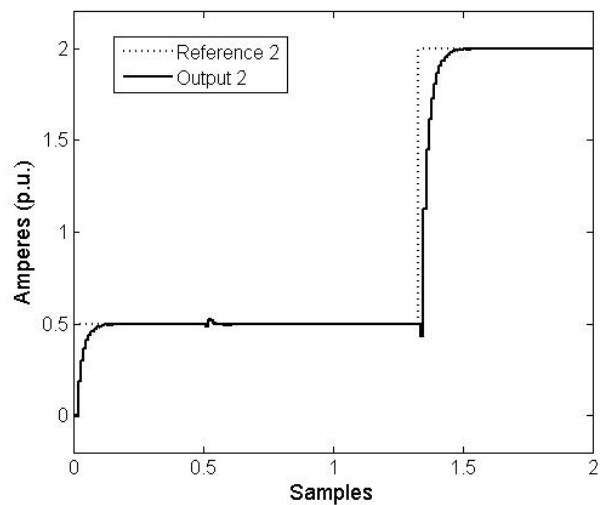


Figure 13. Output 2 tracking performance of MOESP model by using integral multivariable controller.

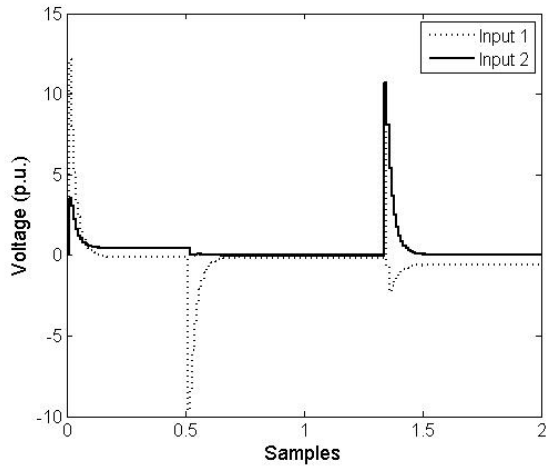


Figure 11. Control signal of ORT model.

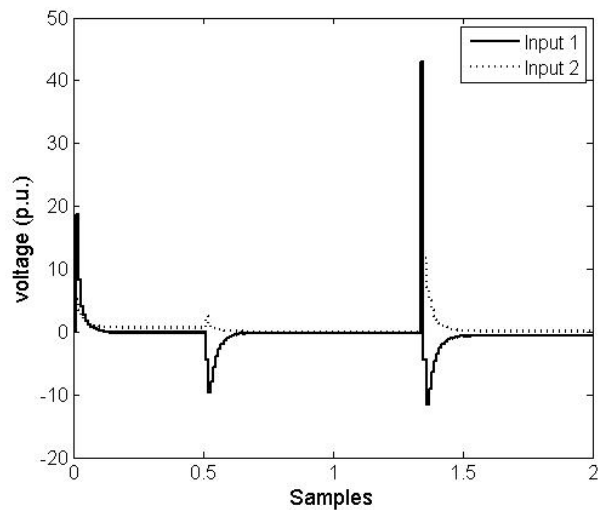


Figure 14. Control signal of MOESP model.

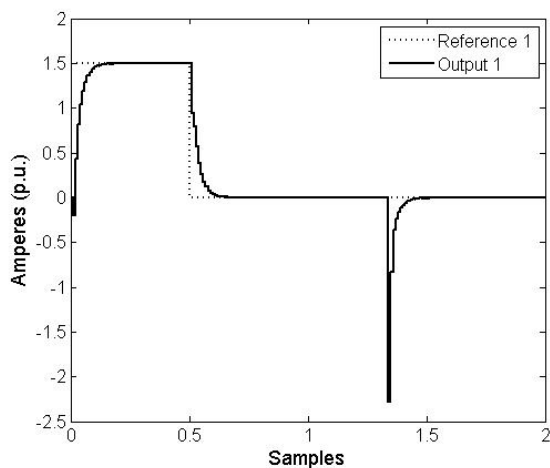


Figure 12. Output 1 tracking performance of MOESP model by using integral multivariable controller.

VI. CONCLUSION AND FUTURE WORK

In this paper, two subspace identification models of a doubly-fed induction generator are obtained based on two subspace algorithms which are ORT and MOESP; they show an advantages when the parameters of system are unknown and are known only the input-output values, because they make it possible to obtain an estimated model of system. The MOESP method gives the best performance overall in open loop compared to the ORT method with the same inputs of real system. However, the output tracking performance by using the ORT model is better than the obtained results with the MOESP model in terms of overshoot and control signal amplitude when it is applied the integral multivariable controller. The settling time in tracking performance in both models is the same.

Since practically many real-world systems are time-varying, the approach proposed in this paper must be considered in order to obtain an approximate model influenced by the behaviour of the system with certain functional characteristics and environmental changes. These simulations can be obtained with a programming tool, like MATLAB/Simulink [12] for testing the results of identification and control algorithms designed before being applied on real-world systems with time-varying.

The proposed methodologies for identification, the MOESP and ORT methods, shown a state space representation of the system without rearranging the estimated parameters in each vector and obtaining the parameters matrices (**A**, **B**, **C** and **D**) with a minor dimensions compared to matrices shown in [13], improving the computational cost with the algorithms.

A future work includes the implementation of algorithms for identification coupled multivariable systems, where couplings are considered between inputs and outputs as possible disturbances present in each subsystem, allow it to obtain an approximate model of system and propose a control strategy of the system.

ACKNOWLEDGMENT

This paper was developed under the research project “Identificación de sistemas multivariables aplicada a generadores eólicos” funded by the Universidad Tecnológica de Pereira with code 6-14-1, and the MSc. thesis “Control óptimo de un sistema multi-variable aplicado a un generador eólico conectado a un sistema de potencia” approved by the “Convocatoria para financiar proyectos de grado de estudiantes de pregrado y posgrado año 2103” funded by the Universidad Tecnológica de Pereira with code E6-14-6.

REFERENCES

- [1] T. Katayama, *Subspace Methods for System Identification*, ser. Communications and Control Engineering, 2006. [retrieved: November, 2014]. [Online]. Available: http://books.google.com.co/books?id=Ge_HTdCBtZAC
- [2] G. Tao, “Recursive Subspace Model Identification Based on Orthogonal Projection and Principal Component Analysis,” in *International Conference on Computer Application and System Modeling (ICCASM 2010)*, Oct 2010, pp. V15-422–V15-429.
- [3] I. W. Jamaludin and N. A. Wahab, “N4SID and MOESP subspace identification methods,” in *9th International Colloquium on Signal Processing and its Applications (CSPA)*, Mar 2013, pp. 140–145.
- [4] D. L. Albarracin-Avila and E. Giraldo, “Adaptive optimal multivariable control of a Permanent Magnet Synchronous Generator,” in *Transmission & Distribution Conference and Exposition - Latin America (PES T&D-LA)*, Sept 2014, pp. 1–5.
- [5] L. Shuhui and T. Haskew, “Energy Capture, Conversion, and Control Study of DFIG Wind Turbine under Weibull Wind Distribution,” in *Power and Energy Society General Meeting PES '09*, Jul 2009, pp. 1–9.
- [6] W. Zhi-nong and Y. Xiao-yong, “The Intelligent Control of DFIG-Based Wind Generation,” in *International Conference on Sustainable Power Generation and Supply (SUPERGEN '09)*, Apr 2009, pp. 1–5.
- [7] H. Jia-bing and Z. Jian Guo, “The internal model current control for wind turbine driven doubly-fed induction generator,” in *Industry Applications Conference, 2006. 41st IAS Annual Meeting. Conference Record of the 2006 IEEE*, Oct 2006, pp. 209–215.
- [8] R. Pena, J. Clare, and G. Asher, “Doubly fed induction generator using back-to-back pwm converters and its application to variable-speed wind-energy generation,” vol. 143, no. 3, May 1996, pp. 231 – 241.
- [9] M. Aziz and R. Mohd-Mokhtar, “Performance Measure of Some Subspace-Based Methods for Closed-Loop System Identification,” in *2nd International Conference on Computational Intelligence, Modelling and Simulation (CIMSIM)*, Sept 2010, pp. 255–260.
- [10] K. H. A.-H. K. Salim, R. and B. Khedjar, “LQR with integral action controller applied to a three-phase three-switch three-level AC/DC converter,” in *IECON 2010 - 36th Annual Conference on IEEE Industrial Electronics Society*, Nov 2010, pp. 550–555.
- [11] D. Giraldo and E. Giraldo, Eds., *Teoría de Control Digital*. Productos Editoriales y Audiovisuales-Produmedios, 2012, ISBN: 978-958-722-151-0.
- [12] S. Karris, *Introduction to Simulink: With Engineering Applications*. Orchard Publications, 2008. [Online]. Available: <https://books.google.com.co/books?id=B8ssmvQmpVoC>
- [13] D. L. Albarracin-Avila and E. Giraldo, “Identification and multivariable control in state space of a permanent magnet synchronous generator,” *TECCIENCIA*, vol. 9, no. 16, pp. 97–106, 2014.